ACS Chemical Neuroscience

pubs.acs.org/chemneuro Letter

Screening and Cellular Characterization of Genetically Encoded Voltage Indicators Based on Near-Infrared Fluorescent Proteins

Mikhail V. Monakhov,[‖] Mikhail E. Matlashov,[‖] Michelangelo Colavita,[‖] Chenchen Song,[‖] Daria M. Shcherbakova, Srdjan D. Antic,* Vladislav V. Verkhusha,* and Thomas Knöpfel*

Cite This: https://dx.doi.org/10.1021/acschemneuro.0c00046 Read Online

ACCESS | Metrics & More | Article Recommendations | Supporting Information

ABSTRACT: We developed genetically encoded voltage indicators using a transmembrane voltage-sensing domain and bright near-infrared fluorescent proteins derived from bacterial phytochromes. These new voltage indicators are excited by 640 nm light and emission is measured at 670 nm, allowing imaging in the near-infrared tissue transparency window. The spectral properties of our new indicators permit seamless voltage imaging with simultaneous blue-green light optogenetic actuator activation as well as simultaneous voltage−calcium imaging when paired with green calcium indicators. Iterative optimizations led to a fluorescent probe, here termed nirButterfly, which reliably reports neuronal activities including subthreshold membrane potential depolarization and hyperpolarization as well as spontaneous spiking or electrically- and optogenetically evoked action potentials. This enables largely improved all-optical causal interrogations of physiology.

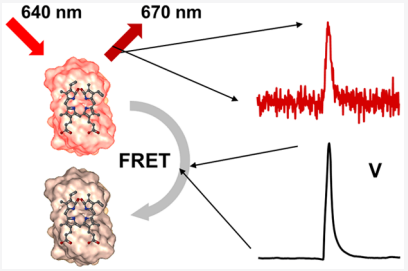

KEYWORDS: *GEVI, Butterfly, biosensor, all-optical electrophysiology, FRET, iRFP*

INTRODUCTION

Development of increasingly better performing genetically encoded voltage indicators (GEVIs) has been ongoing for the last several decades.[1−3] Current GEVIs already allow the direct optical monitoring of fast electrical signals at high spatiotemporal resolution and coverage in vitro and in vivo.[4−12] Like genetically encoded calcium indicators (GECIs), GEVIs enable cell class specific large-scale mapping of neuronal activities in vivo.[1,13−17] In contrast to GECIs, GEVIs are able to report not only action potentials but also depolarizing subthreshold potentials and hyperpolarizing (inhibitory) potentials that underlie information processing at the neuronal level. GEVIs also supersede classic voltage-sensitive dyes, which are difficult to target to specific cell classes and require invasive staining procedures. GEVI-based voltage imaging therefore offers enormous potential for delineating functional electrical processing mechanisms in neurophysiology. However, at the current stage of development, the number of the GEVI-based imaging applications in experimental neuroscience is significantly smaller than the number of the GECI-based applications, due to various limitations of GEVIs, among which a small GEVI signal-to-noise ratio is the most prominent limitation.

Historically, first GEVIs relied on green, cyan, and yellow fluorescent proteins as fluorophores. However, indicators with excitation and emission spectra in near-infrared region are preferred for imaging in vivo since both absorbance and scattering of light in tissue are lowest at 650−900 nm.[18] For imaging in this spectral region, or close to it, several red-shifted indicators were developed. Opsin-based GEVIs such as QuasAr[19] and Archon[20] emit at around 720 nm and have large fractional response but require high excitation light intensities to achieve good signal-to-noise ratio. Thus, their application is limited by the requirement of very intense light sources and concerns for tissue heating.[21] Sensors based on Forster resonance energy transfer (FRET) between rhodopsin and synthetic dyes, such as Voltron[11] and FlareFRET,[22] are bright but their utility is limited by the complexity, outcomes, and risks accompanying dye injection procedures. Sensors based on FRET between rhodopsin and a fluorescent protein, such as Varnam,[9] Ace-mScarlet,[23] and Ace(D81S)-mRuby4,[24] do not require exogenous fluorophores. However, all sensors that rely on energy transfer to rhodopsin from another fluorophore are limited by the rhodopsin absorbance spectrum that does not permit efficient FRET from donors with an emission peak beyond 600 nm. One exception is the Ace-L1-AF594 sensor based on FRET between AF594 dye (emission maximum at 618 nm) and Ace rhodopsin, which has reasonable voltage sensitivity (Table 1) but was not able to detect action potentials in neurons.[22] In contrast, a red-shifted GEVI, FlicR1,[25] does not rely on FRET to rhodopsin, but it emits around 592−605 nm, not reaching the near-infrared tissue transparency window (~640−900 nm).

Received: January 27, 2020
Accepted: October 9, 2020

Table 1. Main Characteristics of Current GEVIs with Excitation >550 nm[a]

GEVI name	excitation peak, nm	emission peak, nm	quantum yield, %	brightness[b]	ΔF/F, % per 100 mV	ΔF/F, % per AP
Ilmol[29]	554[c]	581[c]	69[c]	1889	−4.2	−1.5
FlicR1[30]	570	597	49[c]	1458	9	3
Varnam[9]	558[c]	592[c]	45[c]	2286	−12	−8.4
Ace(D81S)-mRuby4[24]	558	592	45	2357	−9	−3.6
Ace-7aa-mScarlet[23]	569[c]	594[c]	70[c]	2778	14.9	−7.6
Ace-L1-AF594[22]	592[c]	618[c]	66[c]	2410	−23.9	not measured
$Voltron_{635}$[11]	635[c]	652[c]	56[c]	3711	−7	−3
Ace-L1-Cy5 [22]	643[c]	664[c]	27[c]	2679	−5.4	not measured
Arch(D95N)[31]	585	687	0.04	1	50	not reported
QuasAr1[19]	~585	~710	0.8	20	40	20
QuasAr2[19]	~585	~710	0.4	10	90	40−50
Archer1[32]	~585	~710	n/a	10[d]	85	40
Archon1[20]	~585	~710	n/a	28[d]	43	30
Archon2[20]	~585	~710	n/a	80[d]	19	18
SomArchon[17]	~585	~710	n/a	n/a	28	30−40
nirButterfly[this paper]	640	670 (donor), 720 (acceptor)	14	486	−16	−4−8

[a]GEVIs with fluorescence exciation above 550 nm are listed. [b]The values of molecular brightness (unless noted) relative to molecular brightness of Arch(D95N) (the product of Arch(D95N) exctinction coefficient, 63 000 M^{-1} cm^{-1}, and quantum yield, 0.04%, equals 0.0252). [c]The values for respective fluorophores. [d]Experimentally measured brightness of Archer1 is approximately the same as brightness of Quasar2, while Archon1 is 2.8 times brighter than Quasar2 and Archon2 is 8 times brighter than Quasar2. Notably the brightness and other characteristics of opsin-based sensors have complex dependence on excitation light power and wavelength and our comparison should be interpreted with caution.[20]

Besides the considerations of signal attenuation (due to scattering and absorption), the development of near-infrared indicators is important because most commonly used biosensors and optogenetic actuators rely on blue-green light. New, fully encoded, red-shifted sensors will allow spectral multiplexing with existing blue-green fully encoded actuators and green-orange indicators, either for concurrent measurements of more than one biologically relevant variable (voltage, calcium, neurotransmitter, secondary messengers[26]), concurrent measurements of voltage in more than one cell type, or for simultaneous voltage measurement and control. Observation of responses of two cell types labeled by two spectrally orthogonal voltage indicators (for example, orange FlicR1 for interneurons and near-infrared nirButterfly for pyramidal neurons) and control of defined neuron population activity (excitation or inhibition), is necessary for establishing causal relationships between neuronal circuit mechanisms and behaviors. The combination of spectrally nonoverlapping optogenetic actuators for stimulating neuronal activity (control) and GEVIs for recording the neuronal activity (readout) was termed "all-optical electrophysiology" (AOE).[19] Current AOE offers proof-of-principle but is somewhat limited by the low fluorescence quantum yield (QY) of the optical indicators of the QuasAr/Archon type.[19,20]

To overcome the technical limitations related to low brightness and short emission wavelengths of existing indicators, we used monomeric near-infrared (NIR) fluorescent proteins (FPs) of the miRFP family engineered from bacterial phytochromes, which offer the same spectral range as the opsin-based GEVIs QuasAr[19] and Archon[20] but with much higher QY (i.e., they are "brighter"; Table 1).[18] We anticipated that the segregated spectral ranges of two miRFPs and blue-green light activated optogenetic actuators allow improved AOE. In order to test our new GEVI's potential for AOE, we selected the cation channel opsin CheRiff[19] (Figure 1a), distinguished by fast response, strong photocurrent, and blue-shifted activation spectrum. We aimed to develop a sensor with FRET-based, dual-channel voltage readout, resistant to artifacts from movement and dye fading, with high application potential in biological systems.

RESULTS AND DISCUSSION

We generated NIR GEVIs from voltage sensitive fluorescent protein chimeric Butterfly. Chimeric voltage-sensitive fluorescent protein (VSFP) Butterfly employs a synthetic voltage sensing domain derived from the *Ciona intestinalis* voltage sensing phosphatase[27] and Kv3.1 potassium channel (Ci-VSD).[28] We substituted the Butterfly FRET fluorescent protein (FP) pair with a pair of bacterial phytochrome-derived, near-infrared fluorescent proteins "miRFPs" (miRFP670[18] and miRFP720, FRET donor and FRET acceptor, respectively; Figure 1b). While the emission peak of the former protein (667 nm) belongs to the visible range, we call our indicator "near-infrared" for consistency with published reports.[18] Protein links of various lengths and structure were used for tuning the amplitude and dynamics of the voltage-sensitive optical signal.

Early prototypes of these NIR GEVIs exhibited FRET (Figure 1c) and retained the localized membrane targeting properties from chimeric Butterfly when expressed in cultured human embryonic kidney-293 (HEK293) cells (Figure 2a,b).

Functional testing demonstrated a decrease in donor fluorescence and an increase of acceptor fluorescence upon membrane depolarization of patch-clamped HEK293 cells (Figure 1d, Figure 2c,d). The acceptor signal was substantially smaller than donor signal, and the sensor can be practically used for measuring only the donor signal with a peak at 670 nm. In this sense, we could not achieve dual-channel readout as was planned originally. However, even with a small acceptor response, ratiometric measurements (acceptor/donor) may be more resistant to artifacts from movement. It should be noted that the ratio of two signals generally has higher noise than either of two signals (numerator and denominator), and this

https://dx.doi.org/10.1021/acschemneuro.0c00046
ACS Chem. Neurosci. XXXX, XXX, XXX−XXX

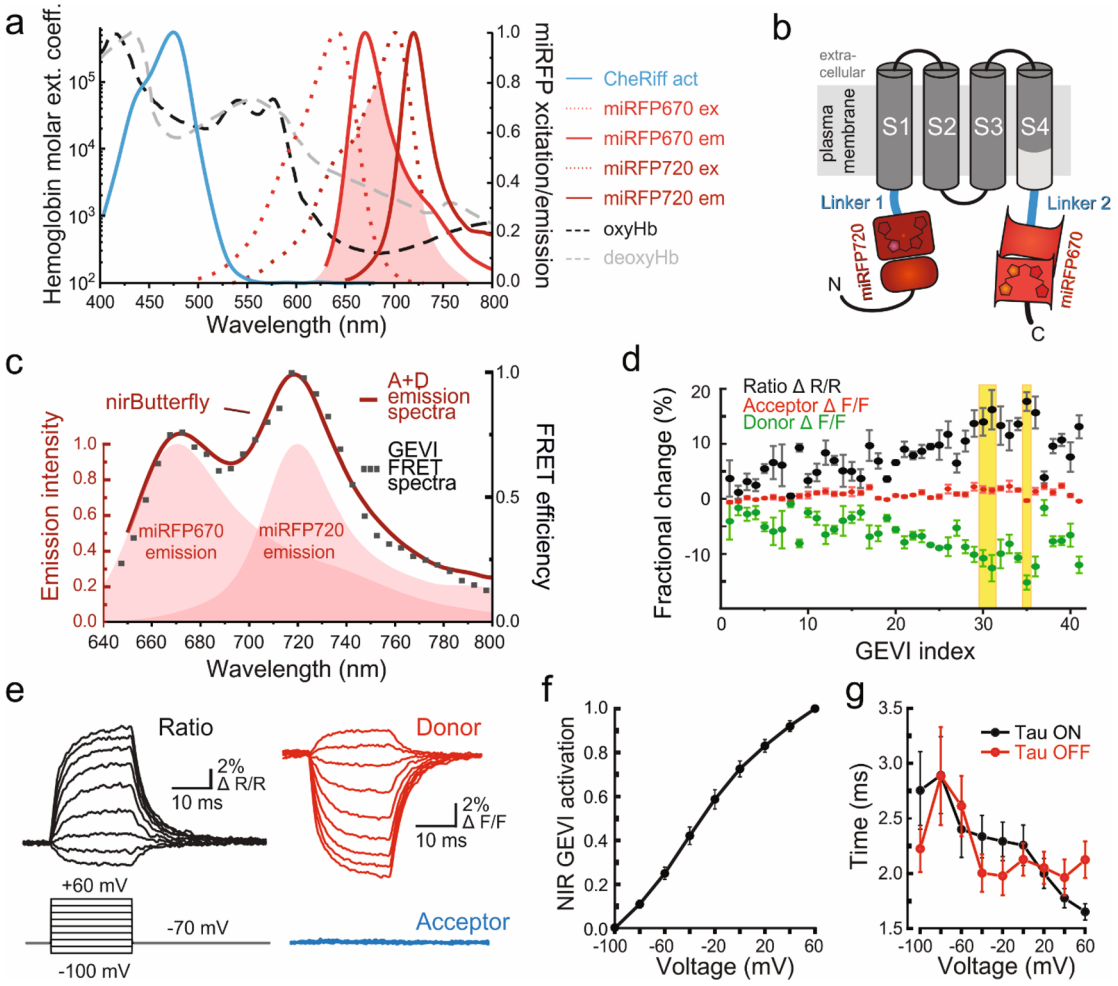

Figure 1. NIR GEVI design and functional characterization. (a) Nonoverlapping spectral compatibility between the excitation (ex) and emission (em) spectra of miRFPs (500−800 nm) with the activation spectrum of the blue-shifted cation channel opsin, CheRiff. Shaded area indicates the overlap integral between miRFP670 (FRET donor) emission and miRFP720 (FRET acceptor) excitation to enable FRET. Spectral bands of miRFPs lie in a region with low extinction coefficient (cm^{-1} M^{-1}) of oxyhemoglobin (oxyHb) and deoxyhemoglobin (deoxyHb). (b) Schematic of the NIR GEVI structural design. A synthetic voltage sensing domain, derived from the *Ciona intestinalis* voltage sensing phosphatase and Kv3.1 potassium channel, is sandwiched between a FRET pair of miRFPs−miRFP670 (donor) and miRFP720 (acceptor). The two linker regions highlighted in blue were varied by mutagenesis toward better performing variants. (c) Emission spectra from nirButterfly (excitation at 633 nm) (black squares) in comparison to the unweighted sum of donor and acceptor emission spectra. (d−g) Functional characterization of NIR GEVIs in voltage clamped HEK293 cells. (d) Evolution of NIR GEVIs. Fluorescence signal amplitudes against index of NIR GEVI variants (index) interactively generated and tested. Yellow shading highlights selected best-performing first generation NIR GEVI variants (NIR GEVI-a, -b, and -c). Henceforth NIR GEVIb is termed "nirButterfly". (e) Representative recording of donor emission, acceptor emission, and fluorescence emission ratio from nirButterfly for a family of voltage steps (20 ms, from −100 mV to +60 mV in 20-mV step size) from a −70 mV holding potential. Average over 10 trials. (f) nirButterfly normalized voltage-activation dependency (N = 15 cells; mean ± SD). (g) nirButterfly ON- and OFF-response time constants, from a single exponential fit (N = 9 cells for τ_{ON}, 8 cells for τ_{OFF}; mean ± SEM; Figure 3).

fact needs to be taken into account when choosing the option to correct for movement-induced signals.

We successively evolved better performing variants (larger dynamic range with fast kinetics) by iterating between patch clamp assay and variations in both the length and amino acid composition of the linker regions between donor FP and VSD as well as between VSD and acceptor FP (Linkers 1 and 2 respectively, Figure 1b,d and Figure 2a). We then selected the three best candidate variants (dubbed "NIR GEVIa", -b, -c, highlighted yellow in Figure 1d) for a more thorough biophysical characterization in HEK293 cells (Figure 1e−g, Figure 3).

In this assay, the fluorescence ratio of NIR GEVIb increased by up to about 8% (5.58% ± 2.16 $\Delta R/R$; mean ± SD, donor −5.13% ± 1.86 $\Delta F/F$, acceptor 0.13% ± 0.14 $\Delta F/F$, N = 11 cells) upon a depolarization step from −80 mV to 20 mV, with an approximately linear relationship between the fluorescence ratio and membrane voltage (Figure 1f). Importantly, the response ON- and OFF-time constants were fast (2.16 ± 0.55 ms, from −70 mV to 0 mV; 2.13 ± 0.42 ms, from 0 mV to −70 mV when fitted with a single exponential time constant; mean ± SD), and time constants were less voltage-dependent than those observed with yellow/red Butterfly[28] (Figure 1g, Figure 3). The fluorescence traces did not exhibit hysteresis previously observed with some opsin-based voltage indicators, where fluorescence changes first reach their peaks and then drop down to their steady-state values[9,11,23,24] (Figure 1e).

Three new constructs, NIR GEVIa, -b, and -c, were then evaluated in neurons of cortical primary cultures. A large fraction of the fluorescence was associated with the plasma

https://dx.doi.org/10.1021/acschemneuro.0c00046
ACS Chem. Neurosci. XXXX, XXX, XXX−XXX

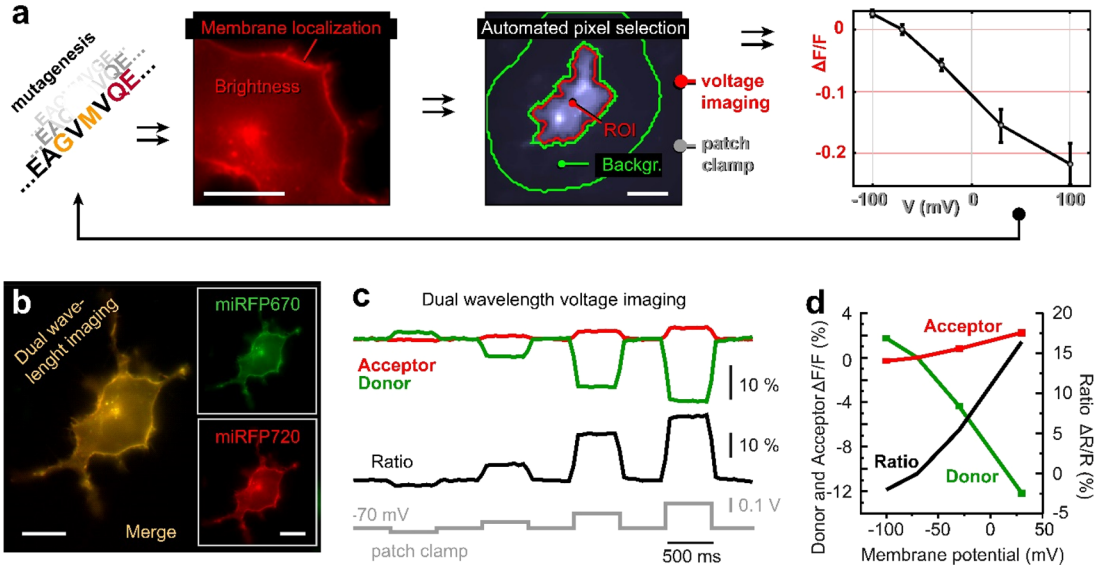

Figure 2. NIR GEVI variant screening in HEK293 cells. (a) The workflow for screening of GEVI variants in HEK293 cells (each loop of the evolutionary process consisted of directed mutagenesis, membrane localization test, followed by simultaneous patch-clamp and fluorescence measurements). Scale bar = 20 μm. Red and green contours indicate automatically selected cell region and background region. (b) NIR GEVI variants retained the localized membrane targeting properties from VSFPs when expressed in cultured HEK293 cells, through both donor (miRFP670) and acceptor (miRFP720) FP channels. Scale bar = 10 μm. (c) In the NIR GEVI screening protocol, selected voltage steps from −70 mV holding potential are applied to the patch-clamped cell, and indicator performance is characterized at two wavelengths. Average of 5 cells. Frame rate 20 Hz. (d) Estimation of fluorescence−voltage relationship for the selected variant at screening.

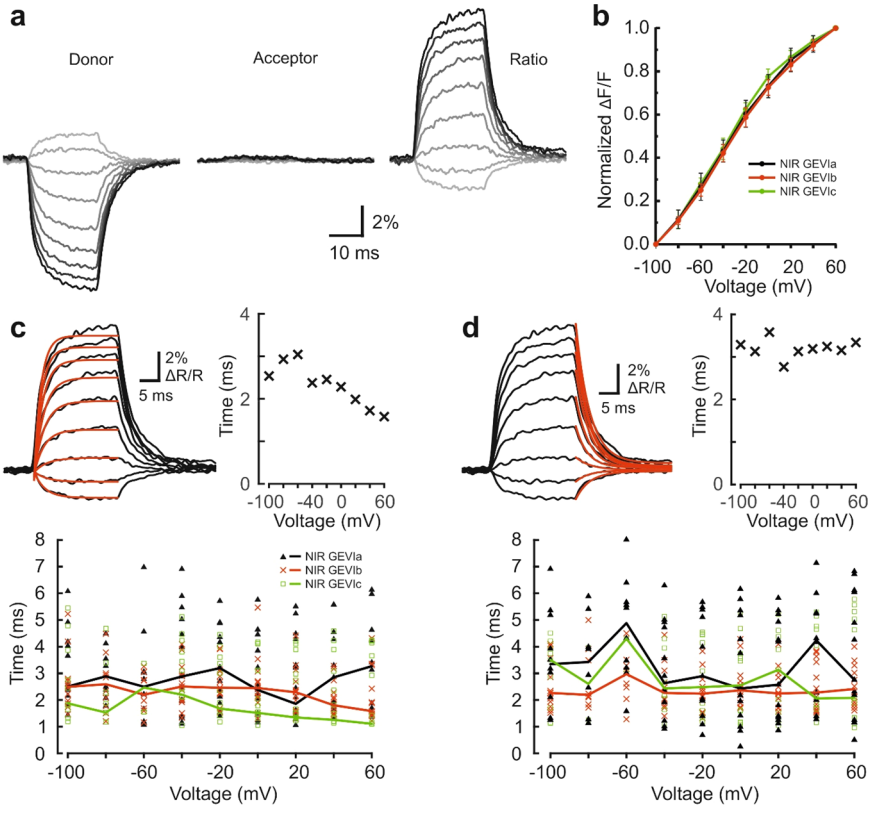

Figure 3. NIR GEVI biophysical characterization in HEK293 cells. (a) Fluorescence response (donor and acceptor $\Delta F/F$; ratio $\Delta R/R$) to the family of voltage steps. Average of 10 trials. (b) Three variants, NIR GEVIa, -b, and -c show similar fluorescence−voltage relationships. Mean ± SD, N = 16 cells for NIR GEVIa, 15 cells for NIR GEVIb, and 11 cells for NIR GEVIc. (c) Upper left: Exponential fitting of the nirButterfly ON-response for estimation of time constants. Upper right: fitted τ_{ON} for a family of voltage steps from a holding potential of −70 mV to step potentials of −100 mV to +60 mV. Lower: Summary of fitted τ_{ON} for NIR GEVIa, -b, and -c. Solid line indicates the median. (d) Same as part c for OFF-response time constants.

https://dx.doi.org/10.1021/acschemneuro.0c00046
ACS Chem. Neurosci. XXXX, XXX, XXX−XXX

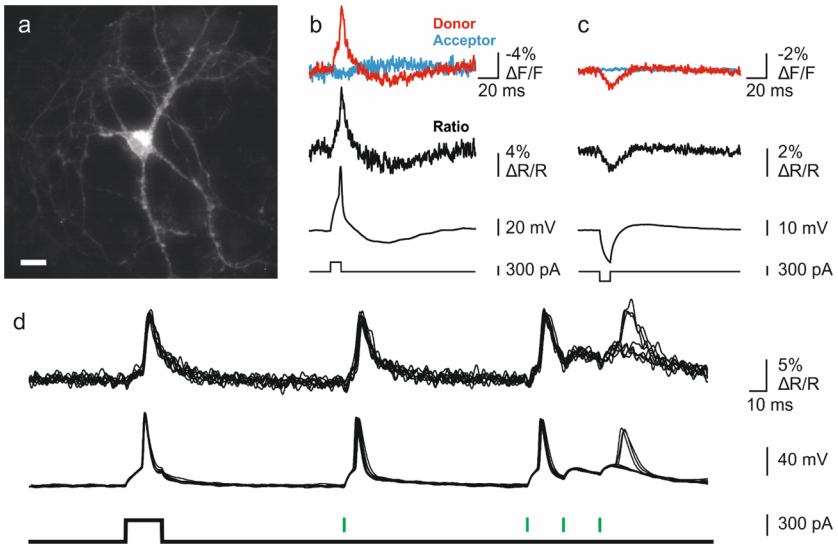

Figure 4. All-optical electrophysiology in neurons. (a) Epifluorescence image of a cultured neuron expressing the voltage sensor, nirButterfly. Scale bar = 10 μm. (b) Optical monitoring of evoked (300 pA current injection) action potential from the current-clamped neuron shown in part a. FRET donor (red) and acceptor (blue) signals provide a ratiometric (middle, black) report of the microelectrode measurements (lower, black) with high fidelity (average of 7 trials shown). (c) NIR GEVI resolves current injection-induced hyperpolarization (average of 20 trials shown). Traces as in part b. (d) Neurons coexpressing nirButterfly and the cation channel opsin CheRiff are used for nirButterfly enabled all-optical electrophysiology. The nirButterfly optical signals resolve action potentials and subthreshold depolarizations induced by either microelectrode current injection or optogenetic light pulse (CheRiff photocurrent). Upper traces show ratio optical signals (eight individual trials superimposed), middle traces show the microelectrode recordings, lower traces show microelectrode (black line) and blue light (green bars) pulses.

membranes both at the soma and at the neurites, although some unwanted intracellular labeling also was present (Figure 4a, Supplementary Figure 1). All three constructs exhibited good voltage sensitivity (NIR GEVIa: 9.3 ± 1.2% $\Delta R/R$/100 mV, donor −8.8 ± 1.2% $\Delta F/F$, acceptor −0.3 ± 0.8% $\Delta F/F$, NIR GEVIb: 10.2 ± 2.6% $\Delta R/R$/100 mV, donor −9.8 ± 2.1% $\Delta F/F$, acceptor −0.6 ± 1.87% $\Delta F/F$, NIR GEVIc 5.6 ± 1.1% $\Delta R/R$/100 mV, −5.3 ± 1.9% $\Delta F/F$, acceptor 0.1 ± 1.2% $\Delta F/F$). We have chosen NIR GEVIb as the most promising variant and termed it "nirButterfly". The nirButterfly sensor reports action potentials and subthreshold membrane potential fluctuations (Figure 4b,c) using relatively modest excitation intensity, not exceeding 50 mW/mm^2, a value much below the average irradiance of near-infrared light routinely used for two photon microscopy (e.g., 1,500 mW/mm^2[17]).

Finally, we have established AOE by cotransfecting cultured cortical neurons with a nirButterfly plasmid and a CheRiff-IRES-NLS-mTagBFP2 plasmid encoding the blue-shifted cation channel opsin variant CheRiff. Like injections of current through a patch clamp electrode, the CheRiff-mediated (photocurrent-triggered) action potentials and subthreshold depolarizations were readily resolved in the optical recording (Figure 4d). Most importantly, the red excitation light used for nirButterfly voltage imaging did not excite CheRiff, hence did not induce any changes in membrane potential, as expected from the complete spectral separation of the actuator opsin (CheRiff) and indicator NIR GEVI (Figure 1a). NIR GEVIs offer sufficient SNR for reliable detection of action potential (Figure 2d, Supplementary Figure 1).

Despite of being brighter than somArchon in identical illumination conditions, the nirButterfly had lower photostability under our measurement conditions (Supplementary Figure 2).

To demonstrate simultaneous measurement of nirButterfly and other spectrally orthogonal probes, we optically recorded from neurons coexpressing voltage indicator, nirButterfly, and a calcium indicator, GCaMP6m. In these experiments, coexpressing neurons were stimulated with voltage pulses via current injection through the patch pipet. In the same experimental trial, nirButterfly reported changes in membrane potential, while GCaMP6m simultaneously reported ensuing rise of intracellular calcium (Supplementary Figure 3).

The nirButterfly performance is commensurable with the best currently available red and NIR GEVIs (for comparison see Table 1) and enables improved AOE, with enhanced quantum yield that allows use of modest red light excitation intensity, suitable for biological applications. Imaging in the NIR spectral range brings two important benefits: (1) A bypass of tissue autofluorescence and hemoglobin signals and (2) an increased tissue penetration for deep-tissue imaging.[33] We expect that nirButterfly will leverage these advantages for in vivo imaging. Potential limitations include dependence on biliverdin as a chromophore. However, near-infrared protein iRFP, an earlier version of fluorescent proteins used in the current study, was successfully imaged in mouse brain,[34] indicating that endogenous biliverdin levels should be sufficient for optical imaging. Compared with opsin-based indicators like Archon, nirButterfly is brighter than somArchon under identical illumination conditions but had lower photostability under our measurement conditions (Supplementary Figure 2). Another limitation, in comparison with opsin-based sensors, is relatively small fractional response. However, at the current performance level, the nirButterfly GEVI might be useful for in vivo population imaging of spontaneous and sensory evoked brain region responses.

The constituent fluorescent proteins miRFP670 and miRFP720 were previously characterized in terms of two-photon excitation.[35] The excitation (cross-sectional values) were highest at 890−950 nm (when measured in the range from 880 to 1300 nm) and the brightness was comparable to

https://dx.doi.org/10.1021/acschemneuro.0c00046
ACS Chem. Neurosci. XXXX, XXX, XXX−XXX

GFP-like proteins. Thus, nirButterfly holds the potential for two-photon imaging. The usage of nirButterfly in dual-indicator (multiplexing) and AOE indicator applications will improve the experimental studies of causal physiological mechanisms in the living systems.

METHODS

Plasmids. Fluorescent proteins used in chimeric VSFP Butterfly[28] were substituted by NIR FPs miRFP670 and miRFP720 [18] at the C- and N-termini (respectively), of the synthetic voltage sensing domain derived from *Ciona intestinalis* voltage sensing phosphatase and Kv3.1 potassium channel (Ci-VSD;[36] Figure 1b). Using this scaffold, a set of constructs with modifications of Linker 1 (between miRFP720 and Ci-VSD) or Linker 2 (between Kv3.1 and miRFP670) were generated either by overlap extension PCR or using site-directed mutagenesis (QuickChange, Agilent, USA). The plasmid (pPuro-CAG-CheRiff-IRES-NLS-mTagBFP2) encoding the optogenetic activating opsin CheRiff was made by subcloning CheRiff, IRES and NLS-mTagBFP2 into pcDNA3.1-Puro-CAG-ASAP vector.

NIR GEVI Screening in HEK Cells. HEK293 cells were maintained in DMEM supplemented with 10% FBS, 2 mM glutamine, 100 U/mL penicillin, and 100 μg/mL streptomycin. Cells were transfected using Lipofectamine 2000 in 24-well plates and were seeded onto poly-D-lysine coated coverslips 2 days after transfection. GEVI testing was performed 1 day after seeding to coverslips. Biliverdin was added 1 day before recording, to a final concentration of 25 μM. Cells were washed with DPBS and placed in the recording chamber with external solution containing (in mM): 125 NaCl, 0.5 KCl, 1 $MgCl_2$, 3 $CaCl_2$, 30 glucose, 1 octanol, and 10 HEPES, pH 7.3, 305 mOsm. Internal solution contained (in mM): 125 K gluconate, 8 NaCl, 0.6 $MgCl_2$, 0.1 $CaCl_2$, 1 EGTA, 4 MgATP, 0.4 NaGTP, and 10 HEPES, pH 7.3, 295 mOsm. Osmolarity was adjusted with sucrose. Glass pipets (1.5/0.75 o.d./i.d.) were pulled with a Flaming/Brown micropipet puller P-97 to a resistance of 6−10 MΩ. Recordings were performed at room temperature. In HEK cells, the voltage was changed (from the holding potential of −70 mV) to −100, −30, 30, and 100 mV in voltage clamp mode using MultiClamp700B amplifier and Digidata1440A digitizer (Molecular Devices, San Jose, CA). The duration of each voltage step and each period between steps was 500 ms. An LED light source with GYR ("Green-Yellow-Red") module was used for excitation of fluorophores (CoolLED, U.K.). Images were acquired using Olympus BX51WI microscope, NeuroCCD camera (gain 30×, 80 × 80 pixels, RedShirtImaging, Decatur, GA), 605/30 nm excitation filter (ET605/30×), 640 nm dichroic mirror (T640lpxr), and emission filters: 667/40 nm (ET667/30m) or 720/40 nm (ET720/40m). $\Delta F/F$ values were calculated for each variant after imaging at frame rate of 20 Hz and kinetics parameters were estimated after imaging at 500 Hz.

Biophysical Characterization of NIR GEVI Variants in HEK Cells. HEK293 cells were transfected with NIR GEVI variants using Lipofectamine, with biliverdin added at time of transfection. Cells were replated on poly-D-lysine coated coverslips at least 8 h after transfection. Whole cell recordings were performed as previously described[4,5] at 32−34 °C, where a family of voltage steps (20 ms; from −100 mV to +60 mV) from −70 mV holding potential was applied to an indicator-expressing voltage-clamped HEK293 cell. Fluorescence was recorded using photodiodes (TILL Photonics, Gräfelfing, Germany) at 10 kHz. The acceptor/donor signal was fitted with a single exponential function for estimation of the ON- and OFF-response time constants.

GEVI FRET spectra was measured using Leica TCS SP5 equipped with 40× (NA 0.85) objective using a 633 nm He−Ne laser for NIR GEVI excitation, fluorescence was imaged in the range of 640 to 800 nm, at 10 nm bandwidth in 5 nm λ steps. ROIs were manually defined over the expressing HEK cells.

Animals. All procedures were in accordance with the UK Animal Scientific Procedures Act (1986) under Home Office Project and Personal Licenses following appropriate ethical review.

Neuronal All-Optical Electrophysiology. Primary cultures of cortical and hippocampal neurons were dissociated from P0.5 C57BL/6 mice and plated onto coverslips precoated with poly-D-lysine and maintained in Neurobasal medium supplemented with 2 mM L-glutamine, 0.5% B-27, and 1% penicillin/streptomycin.[37] Cells were transfected 4 days after plating using calcium phosphate[38] (Invitrogen), and exogenous biliverdin (Sigma) was added 2 days after transfection.

Experiments were performed 14−16 days after transfection. Coverslips with transfected neurons were placed in a recording chamber mounted on the stage of a dual emission widefield epifluorescence immersion microscope (Scientifica, U.K.) and superfused with external solution with the following composition (in mM): 110 NaCl, 3 KCl, 1 $MgSO_4$, 3 $CaCl_2$, 10 glucose, 0.5 Na_2HPO_4, and 10 HEPES, adjusted to pH 7.4 with NaOH (23 °C). Whole-cell current clamp recordings were performed with borosilicate glass pipets (5−7 MΩ) pulled on a two-stage vertical puller (PC-10, Narishige, Japan) and filled with internal solution containing (in mM): 120 K gluconate, 20 KCl, 3 $MgCl_2$, 0.8 $CaCl_2$, 2 EGTA, 4.4 MgATP and 15 HEPES, adjusted to pH 7.3 with KOH. Signals were acquired with an Axon 700B Multiclamp amplifier and digitized at 10 kHz with a Digidata 1440A using pCLAMP software (Molecular Devices, San Jose, CA).

The microscope is equipped with two synchronized CMOS cameras (acA1920-155um, Basler AG) or photodiodes (TILL Photonics, Gräfelfing, Germany), using LED light sources (CoolLED, U.K.; FiberOptoMeter, NPI Electronic, Germany) and the following optical filters (Semrock and Chroma) for NIR GEVI voltage imaging: miRFP670 (donor) excitation FF02-615/20, miRFP670 emission 680/60, miRFP720 emission FF01-775/140, excitation beamsplitter 635LP (FF635-Di01), and detection beamsplitter 700LP (FF700-Di01). CheRiff was activated by blue band-pass filtered (FF01-482/35) LED light, which was combined with the red LED excitation light using a 600 nm long pass dichroic mirror. The longest continuous recording duration was about 30 s.

For expression characterization, cells were fixed using 2% paraformaldehyde after optical imaging experiments and imaged using Leica TCS SP5 equipped with a 63× (NA 1.40) oil immersion objective using 633 nm He−Ne laser for miRFP (NIR GEVI) excitation and 405 nm for NLS-mTagBFP2 (CheRiff) excitation.

Simultaneous Recordings of nirButterfly and GCaMP6m and Comparison of nirButterfly with somArchon. Primary cultures of hippocampal neurons were dissociated from P0-P1 Swiss-Webster mice and plated onto coverslips precoated with poly-D-lysine and maintained in Neurobasal Plus medium supplemented with 1.5 mM GlutaMAX (Gibco), 1% B-27, and 1% penicillin/streptomycin.[37] On DIV10, the neurons were transfected using calcium phosphate[38] (Invitrogen). Experiments were performed 2−3 days after transfection.

For simultaneous optical recording of voltage and calcium activity, the cultured neurons were cotransfected with nirButterfly and calcium indicator GCaMP6m. Exogenous biliverdin (25 μM, Sigma) was added 3 h before recordings. Coverslips with transfected neurons were placed in a recording chamber mounted on the stage of a widefield epifluorescence inverted microscope Olympus IX81 in external solution with the following composition (in mM): 125 NaCl, 2.5 KCl, 1 $MgCl_2$, 3 $CaCl_2$, 10 glucose, and 10 HEPES, adjusted to pH 7.4 with NaOH (23°C). Osmotic pressure was adjusted to 305−310 mOsm with sucrose. Whole-cell current clamp recordings were performed with borosilicate glass pipets (4−7 MΩ) pulled on horizontal puller (P-1000, Sutter Instruments) and filled with internal solution containing (in mM): 125 K gluconate, 8 NaCl, 0.6 $MgCl_2$, 0.1 $CaCl_2$, 1 EGTA, 4 MgATP, 0.4 NaGTP, and 10 HEPES, adjusted to pH 7.3 with KOH. Osmotic pressure was adjusted to 295 mOsm with sucrose.

The microscope was equipped with CMOS camera (Orca Flash LT4.0, Hamamatsu, Japan), UPLFLN40X NA0.75 objective (Olympus), LED light sources with emission maxima at 497 and 617 nm (Mightex, Canada) and the following optical filters (Chroma): nirButterfly (donor) excitation 615/20, emission 667/30, beamsplit-

https://dx.doi.org/10.1021/acschemneuro.0c00046
ACS Chem. Neurosci. XXXX, XXX, XXX−XXX

ter 640LP, GCaMP6m excitation 480/40, emission 535/40, beamsplitter 505LP.

Neurons were patch-clamped and held at −70 mV in voltage clamp mode using Intan CLAMP system (Intan Technologies, CA). A voltage step to +30 mV (duration 4 s) was applied to depolarize the cell and induce calcium influx (command voltage was adjusted to compensate for series resistance).

The motorized microscope allows programmatic control of its Fluorescence Mirror Unit Cassette holding filter cubes for nirButterfly and GCaMP6m in adjacent positions. A custom script was written in Matlab R2018b (MathWorks) using Micro-Manager Core Java API to alternate adjacent filter cubes as fast as possible. At the highest switching rate, the interval between calcium and voltage channels was 2.06 s. Within this period of time the neuron can be recorded for 0.65 s in GCaMP6m channel and then, after switching, for 0.65 s in nirButterfly channel (the remaining 0.76 s are spent on rotation of the filter wheel between two positions).

Two light sources were constantly ON during these optical recordings: 497 nm LED to excite GCaMP6m and 617 nm LED to excite nirButterfly. Throughout the 60 s voltage step protocol, optical imaging was performed using a camera at 20 Hz frame rate. The resulting video consisted of frames taken in "green" channel (with GCaMP6m fluorescence), "red" channel (nirButterfly fluorescence), separated posthoc for GCaMP6m and nirButterfly signals (Supplementary Figure 3).

To compare the brightness and photostability of nirButterfly and somArchon the neurons were transfected to express either protein. Fluorescence was measured with 5 s intervals using 617 nm LED (Mightex, Canada), 620/15× excitation filter, 640LP dichroic mirror, 667/30m emission filter (all from Chroma), and UPLFLN40X NA0.75 objective (Olympus). The irradiance at the sample plane was 44 mW/mm^2. No supplements of respective chromophores were added.

Data Analysis. Optical and electrophysiological signals were analyzed using Clampfit (Molecular Devices) and custom programs under either Matlab 7.4 or Matlab R2018b (MathWorks) and Origin 8 software (OriginLab). Ratiometric calculations were performed as previously described.[4,5] Analysis codes are available upon reasonable request.

■ ASSOCIATED CONTENT

Supporting Information

The Supporting Information is available free of charge at https://pubs.acs.org/doi/10.1021/acschemneuro.0c00046.

> Figures showing confocal image of a neuron expressing nirButterfly, examples of optical traces, comparative analysis of photostability, and an example of simultaneous use of nirButterfly and GCaMP6m in neurons (PDF)

Accession Codes

nirButterfly nucleotide sequence: Genbank MN701056. nirButterfly expression plasmid with CAG promoter: Addgene 136590. nirButterfly expression plasmid with CaMKII promoter: Addgene 136591.

■ AUTHOR INFORMATION

Corresponding Authors

Srdjan D. Antic − *Institute for Systems Genomics, Stem Cell Institute, Department of Neuroscience, UConn Health, Farmington, Connecticut 06030, United States*; Email: antic@uchc.edu

Vladislav V. Verkhusha − *Department of Anatomy and Structural Biology and Gruss-Lipper Biophotonics Center, Albert Einstein College of Medicine, Bronx, New York 10461, United States*; Email: vladislav.verkhusha@einsteinmed.org

Thomas Knöpfel − *Laboratory for Neuronal Circuit Dynamics, Imperial College London, London W12 0NN, U.K.*; Email: t.knopfel@imperial.ac.uk

Authors

Mikhail V. Monakhov − *Institute for Systems Genomics, Stem Cell Institute, Department of Neuroscience, UConn Health, Farmington, Connecticut 06030, United States; Department of Anatomy and Structural Biology and Gruss-Lipper Biophotonics Center, Albert Einstein College of Medicine, Bronx, New York 10461, United States*; orcid.org/0000-0003-0285-2293

Mikhail E. Matlashov − *Department of Anatomy and Structural Biology and Gruss-Lipper Biophotonics Center, Albert Einstein College of Medicine, Bronx, New York 10461, United States*

Michelangelo Colavita − *Laboratory for Neuronal Circuit Dynamics, Imperial College London, London W12 0NN, U.K.*

Chenchen Song − *Laboratory for Neuronal Circuit Dynamics, Imperial College London, London W12 0NN, U.K.*

Daria M. Shcherbakova − *Department of Anatomy and Structural Biology and Gruss-Lipper Biophotonics Center, Albert Einstein College of Medicine, Bronx, New York 10461, United States*

Complete contact information is available at: https://pubs.acs.org/10.1021/acschemneuro.0c00046

Author Contributions

‖M.V.M., M.E.M., M.C., and C.S. had equal contribution. All authors collaborated on the protein design. M.V.M., M.E.M., D.M.S., C.S., and M.C. performed the molecular cloning, GEVI evolution, biophysical characterization, and neurophysiological experiments. T.K., V.V.V., and S.D.A. directed the research. C.S., M.V.M., and T.K. wrote the manuscript. All authors reviewed the manuscript.

Notes

The authors declare no competing financial interest.

Data are available from the corresponding authors upon reasonable request.

■ ACKNOWLEDGMENTS

We thank all members of the Knöpfel, Verkhusha, and Antic laboratories for the useful discussions and suggestions. We thank Adam Cohen for the CheRiff spectra. This work was supported by the Grants NS099573, MH109091, NS103573, and GM122567 from the National Institutes of Health.

■ REFERENCES

(1) Knopfel, T. (2012) Genetically encoded optical indicators for the analysis of neuronal circuits. *Nat. Rev. Neurosci. 13* (10), 687−700.

(2) Lin, M. Z., and Schnitzer, M. J. (2016) Genetically encoded indicators of neuronal activity. *Nat. Neurosci. 19* (9), 1142−53.

(3) Antic, S. D., Empson, R. M., and Knopfel, T. (2016) Voltage imaging to understand connections and functions of neuronal circuits. *J. Neurophysiol. 116* (1), 135−52.

(4) Akemann, W., Mutoh, H., Perron, A., Park, Y. K., Iwamoto, Y., and Knopfel, T. (2012) Imaging neural circuit dynamics with a voltage-sensitive fluorescent protein. *J. Neurophysiol. 108* (8), 2323−37.

(5) Akemann, W., Mutoh, H., Perron, A., Rossier, J., and Knopfel, T. (2010) Imaging brain electric signals with genetically targeted voltage-sensitive fluorescent proteins. *Nat. Methods 7* (8), 643−9.

(6) Yang, H. H., St-Pierre, F., Sun, X., Ding, X., Lin, M. Z., and Clandinin, T. R. (2016) Subcellular Imaging of Voltage and Calcium Signals Reveals Neural Processing In Vivo. *Cell 166* (1), 245−57.

(7) Gong, Y., Huang, C., Li, J. Z., Grewe, B. F., Zhang, Y., Eismann, S., and Schnitzer, M. J. (2015) High-speed recording of neural spikes in awake mice and flies with a fluorescent voltage sensor. *Science 350* (6266), 1361−6.
(8) Platisa, J., Vasan, G., Yang, A., and Pieribone, V. A. (2017) Directed Evolution of Key Residues in Fluorescent Protein Inverses the Polarity of Voltage Sensitivity in the Genetically Encoded Indicator ArcLight. *ACS Chem. Neurosci. 8* (3), 513−523.
(9) Kannan, M., Vasan, G., Huang, C., Haziza, S., Li, J. Z., Inan, H., Schnitzer, M. J., and Pieribone, V. A. (2018) Fast, in vivo voltage imaging using a red fluorescent indicator. *Nat. Methods 15* (12), 1108−1116.
(10) Abdelfattah, A. S., Kawashima, T., Singh, A., Novak, O., Liu, H., Shuai, Y., Huang, Y.-C., Campagnola, L., Seeman, S. C., Yu, J., Zheng, J., Grimm, J. B., Patel, R., Friedrich, J., Mensh, B. D., Paninski, L., Macklin, J. J., Murphy, G. J., Podgorski, K., Lin, B.-J., Chen, T.-W., Turner, G. C., Liu, Z., Koyama, M., Svoboda, K., Ahrens, M. B., Lavis, L. D., and Schreiter, E. R. (2019) Bright and photostable chemigenetic indicators for extended in vivo voltage imaging. *Science 365* (6454), 699.
(11) Abdelfattah, A. S., Valenti, R., Zheng, J., Wong, A., GENIE Project Team, Podgorski, K., Koyama, M., Kim, D. S., and Schreiter, E. R. (2020) A general approach to engineer positive-going eFRET voltage indicators. *Nat. Commun. 11*, 3444.
(12) Knöpfel, T., and Song, C. (2019) Optical voltage imaging in neurons: moving from technology development to practical tool. *Nat. Rev. Neurosci. 20* (12), 719−727.
(13) Carandini, M., Shimaoka, D., Rossi, L. F., Sato, T. K., Benucci, A., and Knopfel, T. (2015) Imaging the awake visual cortex with a genetically encoded voltage indicator. *J. Neurosci. 35* (1), 53−63.
(14) Madisen, L., Garner, A. R., Shimaoka, D., Chuong, A. S., Klapoetke, N. C., Li, L., van der Bourg, A., Niino, Y., Egolf, L., Monetti, C., Gu, H., Mills, M., Cheng, A., Tasic, B., Nguyen, T. N., Sunkin, S. M., Benucci, A., Nagy, A., Miyawaki, A., Helmchen, F., Empson, R. M., Knopfel, T., Boyden, E. S., Reid, R. C., Carandini, M., and Zeng, H. (2015) Transgenic mice for intersectional targeting of neural sensors and effectors with high specificity and performance. *Neuron 85* (5), 942−58.
(15) Allen, W. E., Kauvar, I. V., Chen, M. Z., Richman, E. B., Yang, S. J., Chan, K., Gradinaru, V., Deverman, B. E., Luo, L., and Deisseroth, K. (2017) Global Representations of Goal-Directed Behavior in Distinct Cell Types of Mouse Neocortex. *Neuron 94* (4), 891−907.
(16) Adam, Y., Kim, J. J., Lou, S., Zhao, Y., Xie, M. E., Brinks, D., Wu, H., Mostajo-Radji, M. A., Kheifets, S., Parot, V., Chettih, S., Williams, K. J., Gmeiner, B., Farhi, S. L., Madisen, L., Buchanan, E. K., Kinsella, I., Zhou, D., Paninski, L., Harvey, C. D., Zeng, H., Arlotta, P., Campbell, R. E., and Cohen, A. E. (2019) Voltage imaging and optogenetics reveal behaviour-dependent changes in hippocampal dynamics. *Nature 569* (7756), 413−417.
(17) Piatkevich, K. D., Bensussen, S., Tseng, H. A., Shroff, S. N., Lopez-Huerta, V. G., Park, D., Jung, E. E., Shemesh, O. A., Straub, C., Gritton, H. J., Romano, M. F., Costa, E., Sabatini, B. L., Fu, Z., Boyden, E. S., and Han, X. (2019) Population imaging of neural activity in awake behaving mice. *Nature 574*, 413−417.
(18) Shcherbakova, D. M., Baloban, M., Emelyanov, A. V., Brenowitz, M., Guo, P., and Verkhusha, V. V. (2016) Bright monomeric near-infrared fluorescent proteins as tags and biosensors for multiscale imaging. *Nat. Commun. 7*, 12405.
(19) Hochbaum, D. R., Zhao, Y., Farhi, S. L., Klapoetke, N., Werley, C. A., Kapoor, V., Zou, P., Kralj, J. M., Maclaurin, D., Smedemark-Margulies, N., Saulnier, J. L., Boulting, G. L., Straub, C., Cho, Y. K., Melkonian, M., Wong, G. K., Harrison, D. J., Murthy, V. N., Sabatini, B. L., Boyden, E. S., Campbell, R. E., and Cohen, A. E. (2014) All-optical electrophysiology in mammalian neurons using engineered microbial rhodopsins. *Nat. Methods 11* (8), 825−33.
(20) Piatkevich, K. D., Jung, E. E., Straub, C., Linghu, C., Park, D., Suk, H. J., Hochbaum, D. R., Goodwin, D., Pnevmatikakis, E., Pak, N., Kawashima, T., Yang, C. T., Rhoades, J. L., Shemesh, O., Asano, S., Yoon, Y. G., Freifeld, L., Saulnier, J. L., Riegler, C., Engert, F., Hughes, T., Drobizhev, M., Szabo, B., Ahrens, M. B., Flavell, S. W., Sabatini, B. L., and Boyden, E. S. (2018) A robotic multidimensional directed evolution approach applied to fluorescent voltage reporters. *Nat. Chem. Biol. 14*, 352−360.
(21) Lou, S., Adam, Y., Weinstein, E. N., Williams, E., Williams, K., Parot, V., Kavokine, N., Liberles, S., Madisen, L., Zeng, H., and Cohen, A. E. (2016) Genetically Targeted All-Optical Electrophysiology with a Transgenic Cre-Dependent Optopatch Mouse. *J. Neurosci. 36* (43), 11059−11073.
(22) Xu, Y., Peng, L., Wang, S., Wang, A., Ma, R., Zhou, Y., Yang, J., Sun, D. E., Lin, W., Chen, X., and Zou, P. (2018) Hybrid Indicators for Fast and Sensitive Voltage Imaging. *Angew. Chem., Int. Ed. 57* (15), 3949−3953.
(23) Beck, C., and Gong, Y. (2019) A high-speed, bright, red fluorescent voltage sensor to detect neural activity. *Sci. Rep. 9*, 15878.
(24) Xu, Y., Deng, M., Zhang, S., Yang, J., Peng, L., Chu, J., and Zou, P. (2019) Imaging Neuronal Activity with Fast and Sensitive Red-Shifted Electrochromic FRET Indicators. *ACS Chem. Neurosci. 10* (12), 4768−4775.
(25) Abdelfattah, A. S., Farhi, S. L., Zhao, Y., Brinks, D., Zou, P., Ruangkittisakul, A., Platisa, J., Pieribone, V. A., Ballanyi, K., Cohen, A. E., and Campbell, R. E. (2016) A Bright and Fast Red Fluorescent Protein Voltage Indicator That Reports Neuronal Activity in Organotypic Brain Slices. *J. Neurosci. 36* (8), 2458.
(26) Qian, Y., Piatkevich, K. D., Mc Larney, B., Abdelfattah, A. S., Mehta, S., Murdock, M. H., Gottschalk, S., Molina, R. S., Zhang, W., Chen, Y., Wu, J., Drobizhev, M., Hughes, T. E., Zhang, J., Schreiter, E. R., Shoham, S., Razansky, D., Boyden, E. S., and Campbell, R. E. (2019) A genetically encoded near-infrared fluorescent calcium ion indicator. *Nat. Methods 16* (2), 171−174.
(27) Murata, Y., Iwasaki, H., Sasaki, M., Inaba, K., and Okamura, Y. (2005) Phosphoinositide phosphatase activity coupled to an intrinsic voltage sensor. *Nature 435* (7046), 1239−43.
(28) Mishina, Y., Mutoh, H., Song, C., and Knopfel, T. (2014) Exploration of genetically encoded voltage indicators based on a chimeric voltage sensing domain. *Front. Mol. Neurosci. 7*, 78.
(29) Yi, B., Kang, B. E., Lee, S., Braubach, S., and Baker, B. J. (2018) A dimeric fluorescent protein yields a bright, red-shifted GEVI capable of population signals in brain slice. *Sci. Rep. 8*, 15199.
(30) Abdelfattah, A. S., Farhi, S. L., Zhao, Y., Brinks, D., Zou, P., Ruangkittisakul, A., Platisa, J., Pieribone, V. A., Ballanyi, K., Cohen, A. E., and Campbell, R. E. (2016) A Bright and Fast Red Fluorescent Protein Voltage Indicator That Reports Neuronal Activity in Organotypic Brain Slices. *J. Neurosci. 36* (8), 2458−72.
(31) Kralj, J. M., Douglass, A. D., Hochbaum, D. R., Maclaurin, D., and Cohen, A. E. (2012) Optical recording of action potentials in mammalian neurons using a microbial rhodopsin. *Nat. Methods 9* (1), 90−95.
(32) Flytzanis, N. C., Bedbrook, C. N., Chiu, H., Engqvist, M. K., Xiao, C., Chan, K. Y., Sternberg, P. W., Arnold, F. H., and Gradinaru, V. (2014) Archaerhodopsin variants with enhanced voltage-sensitive fluorescence in mammalian and Caenorhabditis elegans neurons. *Nat. Commun. 5*, 4894.
(33) Xu, Y., Zou, P., and Cohen, A. E. (2017) Voltage imaging with genetically encoded indicators. *Curr. Opin. Chem. Biol. 39*, 1−10.
(34) Tran, M. T. N., Tanaka, J., Hamada, M., Sugiyama, Y., Sakaguchi, S., Nakamura, M., Takahashi, S., and Miwa, Y. (2014) In vivo image analysis using iRFP transgenic mice. *Exp. Anim. 63* (3), 311−319.
(35) Piatkevich, K. D., Suk, H. J., Kodandaramaiah, S. B., Yoshida, F., DeGennaro, E. M., Drobizhev, M., Hughes, T. E., Desimone, R., Boyden, E. S., and Verkhusha, V. V. (2017) Near-Infrared Fluorescent Proteins Engineered from Bacterial Phytochromes in Neuroimaging. *Biophys. J. 113* (10), 2299−2309.
(36) Mishina, Y., Mutoh, H., and Knopfel, T. (2012) Transfer of Kv3.1 voltage sensor features to the isolated Ci-VSP voltage-sensing domain. *Biophys. J. 103* (4), 669−76.

https://dx.doi.org/10.1021/acschemneuro.0c00046
ACS Chem. Neurosci. XXXX, XXX, XXX−XXX

(37) Beaudoin, G. M., 3rd, Lee, S. H., Singh, D., Yuan, Y., Ng, Y. G., Reichardt, L. F., and Arikkath, J. (2012) Culturing pyramidal neurons from the early postnatal mouse hippocampus and cortex. *Nat. Protoc.* *7* (9), 1741−54.
(38) Jiang, M., and Chen, G. (2006) High Ca2+-phosphate transfection efficiency in low-density neuronal cultures. *Nat. Protoc.* *1* (2), 695−700.

https://dx.doi.org/10.1021/acschemneuro.0c00046
ACS Chem. Neurosci. XXXX, XXX, XXX−XXX